

A Case Study of the the Impact of AIRS Temperature Retrievals on Numerical Weather Prediction

O. Reale, ¹, R. Atlas and J.C. Jusem ².

NASA Goddard Space Flight Center, Laboratory for Atmospheres, Greenbelt, Maryland, USA.

Large errors in numerical weather prediction are often associated with explosive cyclogenesis. Most studies focus on the under-forecasting error, i.e. cases of rapidly developing cyclones which are poorly predicted in numerical models. However, the over-forecasting error (i.e., to predict an explosively developing cyclone which does not occur in reality) is a very common error that severely impacts the forecasting skill of all models and may also present economic costs if associated with operational forecasting. Unnecessary precautions taken by marine activities can result in severe economic loss. Moreover, frequent occurrence of over-forecasting can undermine the reliance on operational weather forecasting. Therefore, it is important to understand and reduce the predictions of extreme weather associated with explosive cyclones which do not actually develop.

In this study we choose a very prominent case of over-forecasting error in the northwestern Pacific. A 960 hPa cyclone develops in less than 24 hour in the 5-day forecast, with a deepening rate of about 30 hPa in one day. The cyclone is not verified in the analyses and is thus a case of severe over-forecasting.

By assimilating AIRS data, the error is largely eliminated. By following the propagation of the anomaly that generates the spurious cyclone, it is found that a small mid-tropospheric geopotential height negative anomaly over the northern part of the Indian subcontinent in the initial conditions, propagates westward, is amplified by orography, and generates a very intense jet streak in the subtropical jet stream, with consequent explosive cycloge-

¹Additional Affiliation: University of Maryland, Baltimore County, Baltimore, Maryland, USA

²Additional Affiliation: Science Application International Corporation, Beltsville, Maryland, USA

nesis over the Pacific. The AIRS assimilation eliminates this anomaly that may have been caused by erroneous upper-air data, and represents the jet stream more correctly. The energy associated with the jet is distributed over a much broader area and as a consequence a multiple, but much more moderate cyclogenesis is observed.

A Case Study of the Impact of AIRS Temperature Retrievals on Numerical Weather Prediction

O. Reale,^{1,2} R. Atlas,¹ and J. C. Jusem^{1,3}

Abstract. Large errors in numerical weather prediction are often associated with explosive cyclogenesis. Most studies focus on the under-forecasting error, i.e. cases of rapidly developing cyclones which are poorly predicted in numerical models. However, the over-forecasting error (i.e., the prediction of an explosively developing cyclone which does not occur in reality) is a very common error that severely impacts the forecasting skill of all models and may also present economic costs if associated with operational forecasting. Unnecessary precautions taken by marine activities can result in severe economic loss. Moreover, frequent occurrence of over-forecasting can undermine the reliance on operational weather forecasting. Therefore, it is important to understand and reduce the predictions of extreme weather associated with explosive cyclones which do not actually develop.

In this study we choose a very prominent case of over-forecasting error in the north-western Pacific. A 960 hPa cyclone develops in less than 24 hour in the 5-day forecast, with a deepening rate of about 30 hPa in one day. The cyclone is not verified in the analyses and is thus a case of severe over-forecasting.

By assimilating data from the Atmospheric Infrared Sounder (AIRS) mounted on the NASA's Aqua Spacecraft, the error is largely eliminated. By following the propagation of the anomaly that generates the spurious cyclone, it is found that a small mid-tropospheric geopotential height negative anomaly over the northern part of the Indian subcontinent in the initial conditions, propagates westward, is amplified by orography, and generates a very intense jet streak in the subtropical jet stream, with consequent explosive cyclogenesis over the Pacific. The AIRS assimilation eliminates this anomaly that may have been caused by erroneous upper-air data, and represents the jet stream more correctly. The energy associated with the jet is distributed over a much broader area and as a consequence a multiple, but much more moderate cyclogenesis is observed.

1. Introduction

Explosive cyclogenesis, defined as a cyclone formation in which the deepening rate exceeds 24 hPa in 24 hours, normalized at the latitude of 60°, (Sanders and Gyakum, 1980), occurs frequently in nature and is a major task for numerical forecasting. Over the last 25 years, enormous improvements have been obtained in the forecasting of explosive cyclones. Among the several complex forcings contributing to explosive cyclogenesis (e.g. Bullock and Gyakum, 1993), the role of latent and sensible heat fluxes (e.g. Bosart, 1981) and the role of jet streaks (e.g. Uccellini et al., 1987) have received the greatest attention from the atmospheric modeling community. Satellite information have helped substantially to improve the representation of surface fluxes and of the jet stream, the latter being related to a correct representation of the three-dimensional thermal structure of the atmosphere and to improvements in the analysis of tropopause fold-

¹NASA Goddard Space Flight Center, Laboratory for Atmospheres, Greenbelt, Maryland, USA.

²University of Maryland, Baltimore County, Baltimore, Maryland, USA.

³Science Application International Corporation, Beltsville, Maryland, USA.

ing.

In spite of the improvements, explosive cyclogenesis still represents a challenge even for the current atmospheric models, and explosive cyclones can be totally missed in operational weather forecasts on various ranges. Several studies have considered the so-called 'underforecasting' error, in which the formation of an explosive cyclone or its explosive deepening are not predicted, and have proposed different strategies to improve the forecast of these dangerous storms (e.g., among others, Hello et al., 2000; Leutbecher et al., 2002; Fourrié et al., 2003).

However, even if the increased resolution of global models, the improved representation of sea surface fluxes, and the capability of models' dynamical cores to develop rapidly growing disturbances have reduced the underforecasting error, the reverse problem is being faced even more often: spurious, explosive cyclones develop in the models and are not verified in the analyses. This 'overforecasting' error is most common when the increased capability of global models to represent some of the sub-synoptic scale aspects of explosive cyclogenesis is not matched by an equal improvement in the initialization. The more a model can develop realistically fast growing modes, the more important it becomes to avoid inserting spurious disturbances in the initial conditions.

The overforecasting error severely affects the overall performance of the model, but it has not been systematically studied. It is however a very important error, because it undermines confidence in operational forecasting and is often associated with economic losses, whenever precautions are taken in response to a forecast of an explosive event which does not verify.

In this work, we select a spectacular case of overforecasted cyclogenesis that occurred in a 5-day forecast initialized on 8 January 2003 over the northwestern Pacific. We then perform an assimilation experiment in which AIRS-derived thicknesses profiles are assimilated globally, to improve the vertical temperature structure. In this simulation, the spurious cyclone is completely suppressed. We then compare the dynamical evolution of the two simulations, in order to investigate the physical mechanisms through which the information introduced by the AIRS assimilation propagates in the model.

2. The Model

The model used in this study is the finite-volume General Circulation Model (fvGCM) developed at the NASA Goddard Space Flight Center (GSFC) and based on the finite-volume dynamical core with terrain-following Lagrangian control-volume discretization documented in Lin (2004). The finite-volume dynamical core at NASA GSFC is the result of more than ten years of intense effort, in which the most fundamental steps are:

1. Development of algorithms for transport processes of water vapor (Lin et al., 1994).
2. Development of multi-dimensional "Flux-Form Semi-Lagrangian Transport" scheme (FFSL, Lin and Rood, 1996).
3. Adaptation of the FFSL algorithm to the shallow water dynamical framework (Lin and Rood, 1997).
4. Development of a simple finite-volume integration method for computing pressure gradient in general terrain-following coordinates (Lin, 1997).

The physics parameterizations implemented in this version of the NASA fvGCM are from the the National Center for Atmospheric Research (NCAR) Climate Community Model CCM version 3.6.6 (Kiehl et al., 1998).

In this work, the forecast model is coupled with a sequential analysis system in which the atmospheric state is carried forward in time by the prediction model, and the Kalman filter analysis equation is solved at each synoptic time by the so-called Physical-space Statistical Analysis System (PSAS, Cohn et al. 1998). This system comprised the fvGCM and PSAS is also called the finite-volume Data Assimilation System (fvDAS) and operationally is known as the NASA Goddard Earth Observing System (GEOS). The work described in this article is carried out using version 4.0.3 of the GEOS (equivalent to fvDAS 1.4r2), with the forecast model being run at a horizontal resolution of $1^\circ \times 1.25^\circ$ and 55 layers in the vertical, while the analysis increments are calculated at a resolution of $2^\circ \times 2.5^\circ$ and 25 levels.

3. The Experiment.

3.1. A case study of overforecasting error

The particular formulation of the finite-volume dynamical core enables the model to effectively handle strong gradients, so that fronts and sharp thermal gradients are accurately represented and vorticity is advected very efficiently. However, the initialization is a crucial aspect of the forecasting problem, and a model in which rapid developments are intrinsically possible is often prone to large errors if the initialization is not adequate. One of the typical consequences of less-than-optimal initializations for a model capable of resolving rapid developments, is the creation of spurious rapidly developing cyclones.

In this work, we select a case of severely overforecasted cyclogenesis that occurred over the northwestern Pacific in a 5-day forecast initialized on 8 January 2003. This simulation is defined as the "Control run". We then perform an assimilation experiment in which AIRS-derived thickness profiles are assimilated globally, with the aim of improving the overall vertical thermal structure of the atmosphere. We define this experiment as the "AIRS run".

3.2. Results

In Fig. 1 the sea level pressure (slp) for the two initializations (Control and AIRS) at 0000 UTC 8 January 2003, together with their corresponding 120-hour forecast, are shown. Although relatively small differences due to the assimilation of AIRS data are present, both Figs. 1a,c display a major, large-scale cyclone spanning nearly the entire northern Pacific. This system advects Siberian air over the Kuro-Shio and over most of the northwestern Pacific, and is therefore a major potential source of instability and secondary developments.

In Fig. 1b it can be seen that three smaller-scale cyclones develop in 120 hours out of the large-scale system observed in Fig. 1a; one of these is a very intense, smaller-scale cyclone, with a minimum slp of 960 hPa, located at about $42^\circ N$ and $167^\circ E$. The shading in Fig. 1b represents the slp forecast minus control analyses at the corresponding time, 0000 UTC 13 January 2004. The small-scale intense cyclone does not verify in the analyses: therefore the slp forecast departure from the analyses is extremely large, of the order of 45 hPa over the cyclone center.

Figures 1c,d show that the AIRS run does not predict this spurious explosive cyclone. The slp difference between the AIRS 120-hour forecast and the corresponding analyses at 0000 UTC 13 January is much more modest. Instead of one, very intense cyclone, the AIRS run

produces three weak or moderate cyclones of nearly comparable intensity.

In Figs. 2 the Control and AIRS analyses at 0000 UTC 13 January are shown, together with the NCEP analyses. Comparing them with Fig. 1, it can be noted that instead of the very intense cyclone erroneously predicted in the Control run (Fig. 1b), a very broad but relatively weak cyclonic circulation spans across most of the northern Pacific, a remnant of the very large and intense cyclone observed in Fig. 1a. Within this very large scale cyclonic circulation, three smaller scale and relatively weak or moderate systems can be observed. It is a typical case in which very large-scale baroclinic conditions left by a pre-existing system can provide an environment favorable to intense cyclogenesis, and/or sudden rejuvenation, if the proper forcing occurs. However an erroneous prediction of any cyclogenetic forcing in this environment can trigger rapid unstable responses in the model. This is what happens in the Control run, as it will be discussed later. On the other hand, it can be noted that the 120-hour AIRS forecast (Fig. 1d) produces three smaller-scale, moderate cyclone, in qualitative agreement with the analyses (Figs. 2a,b,c).

In Figs. 2d,e, where the Control and AIRS 120-hour forecasts are compared with their corresponding verifying analyses at 0000 UTC 13 January over the entire Northern Hemisphere, it is important to observe that the spurious cyclone in the Control run is the largest error and no comparable departure can be found in the AIRS simulation.

In Fig. 3 and 4 the anomaly correlation is calculated with respect to slp and 500 hPa geopotential height, using the NCEP analyses for validation. It can be noted that AIRS improves dramatically the performance of the model over the Southern Hemisphere, but the impact is only very slightly positive over the Northern Hemisphere. This is quite remarkable and suggests that the standard statistical performance evaluation can occasionally be misleading. In fact in our case, smaller amplitude but larger-scale errors (cf. Figs. 2d and 2e) occurring in the AIRS run lead to a comparable global anomaly correlation for the two runs, even if the Control run produces an enormous, but localized, overforecasting error. In this work, we focus on the individual spurious explosive cyclone in the Control forecast, and on the dynamical causes of its disappearance from the AIRS simulation.

4. Dynamical considerations

To investigate when the two simulations diverge, we analyze latitudinally averaged 500 hPa geopotential height and slp differences with the aid of Hovmoeller diagrams, on different strips of latitudes, throughout the northern hemisphere. The most significant result is obtained averaging the latitudes between $25^{\circ}N$ and $35^{\circ}N$. In Fig. 5 the Hovmoeller diagram relative to $25^{\circ}N$ to $35^{\circ}N$ of 500 hPa geopotential height and slp difference between the two simulations, AIRS and Control, is shown. A positive geopotential anomaly of the order of 10m, is present in the initial conditions between longitude $80^{\circ}E$ and $90^{\circ}E$ (approximately over the northern part of the Indian subcontinent) and rapidly propagates eastward, doubling in amplitude between 0600 UTC 10 and 0600 UTC 11 January. By the time the anomaly has reached $140^{\circ}E$ (which is over the Pacific Ocean), its amplitude has quadrupled. Associated with this anomaly, two negative anomalies can be seen, moving at the same propagation speed but leading/lagging by approximately 20° of longitude. The most interesting feature is a strong

positive slp anomaly located between the main positive 500 hPa anomaly and the negative anomaly which is ahead of it. The same diagram calculated for difference heights shows a similar behavior between 400 and 650 hPa approximately (not shown).

Since we are displaying the AIRS minus Control difference, the diagram documents that in the initial conditions, the mid-tropospheric geopotential height at about $25 - 35^{\circ}N$ and $80 - 90^{\circ}E$ is lower in the Control than in the AIRS run. This small-scale mid-tropospheric trough present in the Control run amplifies rapidly between $110^{\circ}E$ and $130^{\circ}E$, in correspondence to the discontinuity between East Asia and the Pacific Ocean, which is downstream the Himalayan-Tibetan orographic forcing. A ridging tendency develops downstream of the moving trough. A slp negative anomaly indicates a cyclone in the Control run which should not be present, or should be weaker, in the AIRS run. This slp anomaly is in a tilted position with respect to the trough, indicating baroclinic growth, and rapidly propagates in phase with the trough and the ridge, thus benefiting from mid-tropospheric positive vorticity advection. Since the diagram shows latitudinally averaged values between $25^{\circ}N$ and $35^{\circ}N$, the magnitude of the anomalies are very significant. Moreover, the apparent weakening at the very end of the integration is due, as will be shown later, to a northward shift of the system rather than to a real weakening.

To verify the possibility hinted by the Hovmoeller diagram, in Fig.6 the 500 hPa AIRS minus Control height anomalies are displayed over the areas suggested by Fig. 5. It can be seen that a positive (AIRS minus Control) anomaly is actually present over the northern part of the Indian subcontinent, and propagates eastward throughout southern Asia. The anomaly amplifies between 10 and 11 January, possibly because of the orographic effect of Tibet (cyclonic vorticity tends to be produced downstream of an orographic obstacle). A further deepening, not captured in the Hovmoeller diagram, takes place on the 12th and the 13th, when the wave moves northeastward, thus leaving the $25 - 35^{\circ}N$ averaging latitudinal band.

According to Figs.5 and 6, we should expect a mid-tropospheric shortwave developing in the Control and not developing (or developing less) in the AIRS simulation. In fact, in Fig. 7a,b we can see a small cyclonic vorticity maximum at 0000 UTC 9 January and at about $30 - 35^{\circ}N$ and $90 - 100^{\circ}E$, stronger in the Control than in AIRS. At 0000 UTC 10 January, the vorticity maximum is at about $110^{\circ}E$, in agreement with Fig.5, and at 0000 UTC 11 January, when the strongest development starts to occur, the system is over the land-ocean border. At this time, a clear 500 hPa short wave structure is evident in the Control run.

In Figs. 8 and 9 the slp, 250 hPa wind speed, 500 hPa geopotential height and vorticity are shown, in the Control and AIRS simulations respectively. The longitude of the frame moves eastward to follow the development of the spurious cyclone. In the Control run, the small-scale, intense spurious cyclone develops in an ideal baroclinic way (Figs. 8c,d,e,f) in response of the mid-tropospheric anomaly seen before. The environment over the northern Pacific left by the decay of the very large system in Fig. 1a, is very favorable to intense baroclinic development, so that even a small disturbance like the one seen in Fig. 7e can produce a explosive cyclogenesis. It should be noted that the jet stream is also affected by the mid-tropospheric anomaly. In spite of the fact that no substantial (AIRS minus Control) difference at 250 hPa can be seen in the initial conditions over the area where the

mid-tropospheric discrepancy is found, the spurious development in the Control is associated with an intense jet streak (Fig. 8e), not present in the AIRS run (Fig. 9e). Moreover no evidence of the very intense 500 hPa short-wave can be seen in the AIRS run (cf. Figs. 8d,f with Figs. 9d,f).

5. Conclusions

In this work we analyze a case of major overforecasting error in the NASA finite volume General Circulation Model. A spurious explosive cyclogenesis is produced in the 120-hour forecast. By comparing the model's results with a simulation performed with the same model, in which AIRS-inferred thicknesses are assimilated globally and in which the spurious cyclogenesis does not occur, it is found that the AIRS can correct a height error that probably originated from incorrect upper-air observations over the northern part of the Indian subcontinent. This error causes geopotential height in the initial conditions to be lower of about 10–15 m and because of the particular location (upstream of a major orographic barrier) it propagates as a small trough throughout Asia, is amplified downstream by orography and, finding very favorable conditions over the Pacific for development, originates a very strong cyclone which is not observed in the analyses. The AIRS corrects this error in the initial conditions, and the corresponding simulation is thus not affected by the spurious development.

Acknowledgments. This work was supported by NASA's Office of Earth Science. Eugenia Brin and Dennis Bungato provided computer and graphics support for the AIRS experiments. The authors benefited from discussions with Drs. Joel Susskind and Moustafa Chahine.

References

- Bosart, L. F., 1981: The Presidents' Day snowstorm of 18–19 February 1979: A subsynoptic scale event. *Mon. Wea. Rev.*, **109**, 1542–1566.
- Bullock, T. A., and J. R. Gyakum, 1993: A diagnostic study of cyclogenesis in the western North Pacific Ocean. *Mon. Wea. Rev.*, **121**, 65–75.
- Cohn, Stephen E., Arlindo da Silva, Jing Guo, Meta Sienkiewicz, David Lamich, 1998: Assessing the Effects of Data Selection with the DAO Physical-Space Statistical Analysis System. *Mon. Wea. Rev.*, **126**, 2913–2926.
- Fourrié, N., C. Claud, and A. Chédin, 2003: Depiction of Upper-Level Precursors of the December 1999 Storms from TOVS observations. *Mon. Wea. Rev.*, **131**, 417–430.
- Kiehl, J. T., J. J. Hack, G. B. Bonan, B. A. Boville, D. L. Williamson, and P. J. Rasch, 1998: The National Center for Atmospheric Research Community Climate Model (CCM3). *J. Clim.*, **11**, 1131–1149.
- Hello, G. and F. Lalaurette and J.-N. Thepaut, 2000: Combined use of sensitivity information and observations to improve meteorological forecasts: A feasibility study applied to the 'Christmas storm' case. *Q. J. R. Meteorol. Soc.*, **126**, 621–647.
- Lin, S.-J., and R. B. Rood, 1996: Multidimensional flux-form semi-Lagrangian transport schemes. *Mon. Wea. Rev.*, **124**, 2046–2070.
- Lin, S.-J., 1997: A finite-volume integration method for computing pressure gradient forces in general vertical coordinates. *Q. J. Roy. Met. Soc.*, **123**, 1749–1762.
- Lin, S.-J., and R. B. Rood, 1997: An explicit flux-form semi-Lagrangian shallow water model on the sphere. *Q. J. Roy. Met. Soc.*, **123**, 2477–2498.
- Lin, S.-J., 2003: NASA's high-end atmospheric model for climate and weather predictions, *EOM*, vol. 12, no. 2, 14–18.

- Lin, S.-J., R. Atlas, and K.-S. Yeh, 2004: Global weather prediction and high-end computing at NASA. *Computing in Science and Engineering*, vol. 6, no. 1, p. 29-35.
- Lin, S.-J., 2004: A "vertically Lagrangian" finite-volume dynamical core for global models. *Mon. Wea. Rev.*, *132*, 2293-2307.
- Leutbecher, J. Barkmeijer, T. N. Palmer and A. J. Thorpe, 2002: Potential improvements of forecasts of two severe storms using targeted observations. *Q. J. R. Meteorol. Soc.*, *128*, 105-122.
- Sanders, F., and J. R. Gyakum, 1980: Synoptic-dynamic climatology of the "bomb." *Mon. Wea. Rev.*, *108*, 1589-1606.
- Uccellini, L.W., R. A. Petersen, K. F. Brill, P. J. Kocin and J. J. Tuccillo, 1987: Synergistic interactions between an upper-level jet streak and diabatic processes that influence the development of a low-level jet and a secondary coastal cyclone. *Mon. Wea. Rev.*, *115*, 2227-2261.

O. Reale, Laboratory for Atmospheres, Code 910, NASA
Goddard Space Flight Center, Greenbelt, MD 20771, USA.
(Oreste.Reale.1@gsfc.nasa.gov)

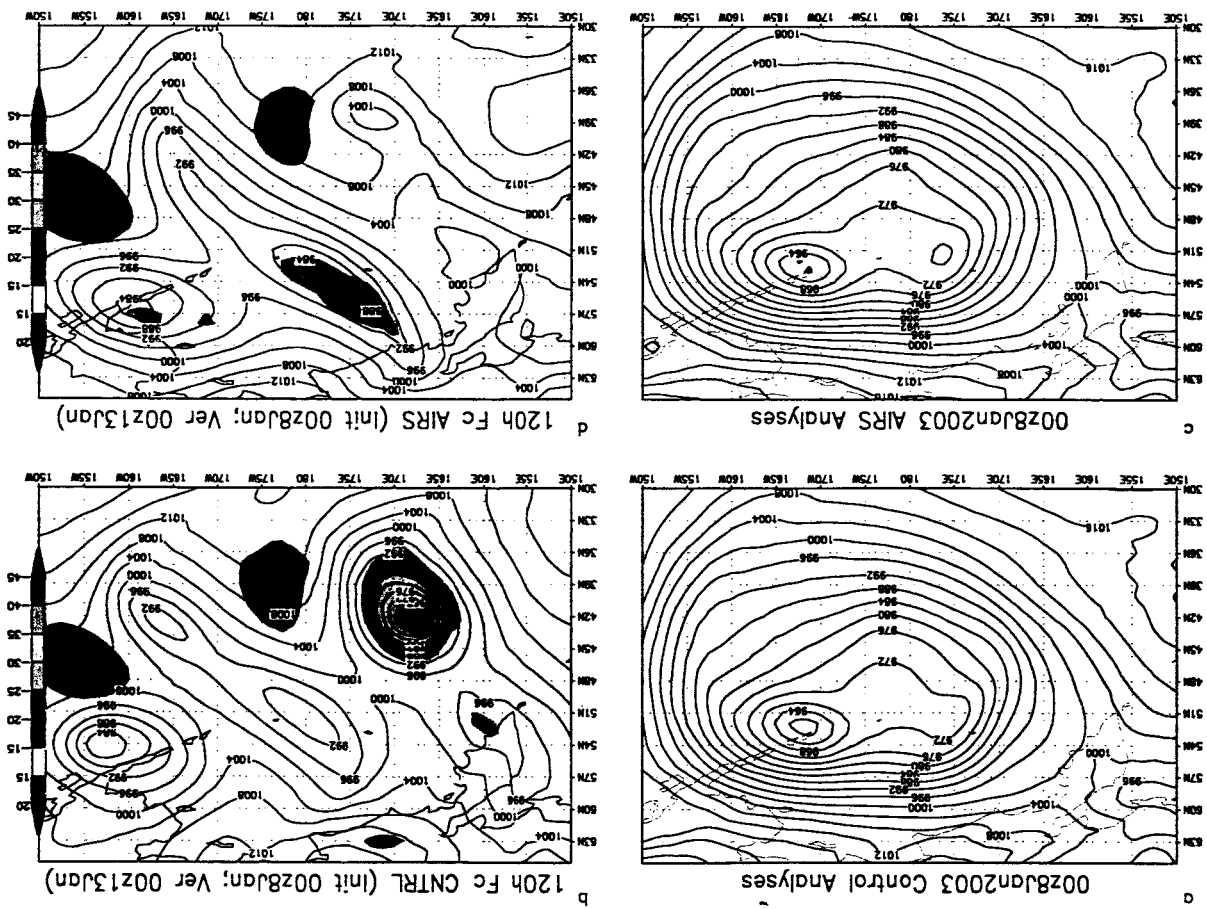
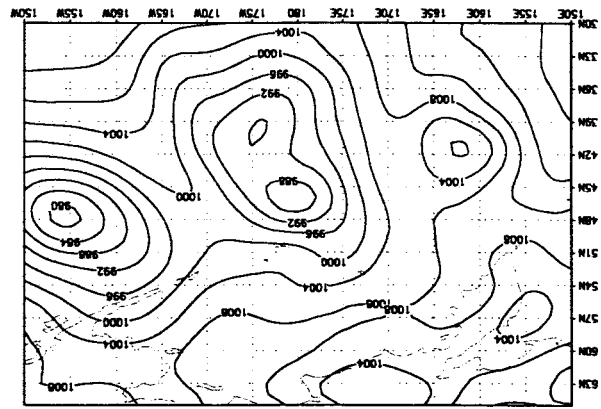
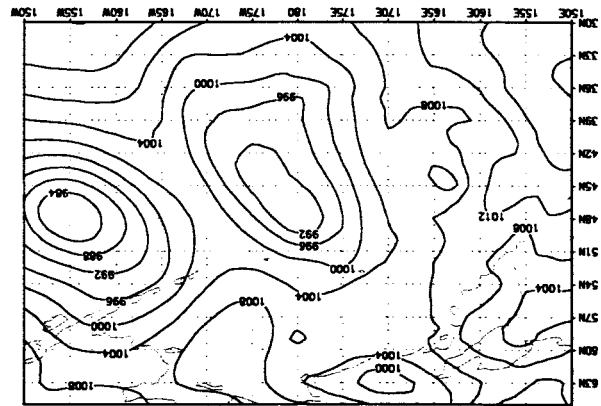


Figure 1. Sea level pressure (hPa). (a) 0000 UTC 8 January 2003 Control analyses. (b) 120-hour Control forecast (solid line) for 0000 UTC 13 January 2003 and difference between the forecast and corresponding Control verifying analyses (shaded). (c) 0000 UTC 8 January 2003 AIRS verifying analyses (solid line) for 0000 UTC 13 January 2003 and difference between the forecast and corresponding AIRS verifying analyses (shaded).

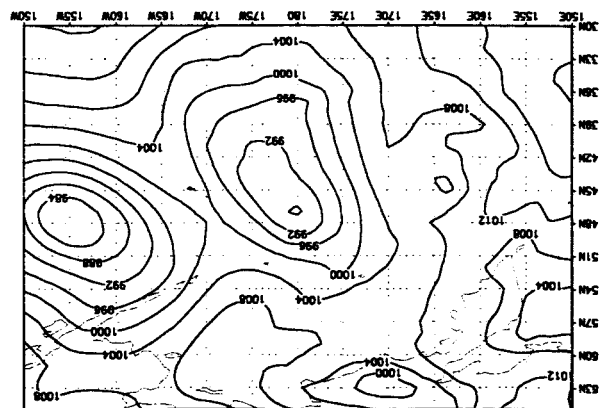
Figure 2. Left panels: sea level analyses pressure at 0000 UTC 13 January (hPa): (a) Control; (b) AIRS; (c) NCEP. Right panels: 120 hour forecast minus corresponding verifying analyses. (d) Control; (e) AIRS.



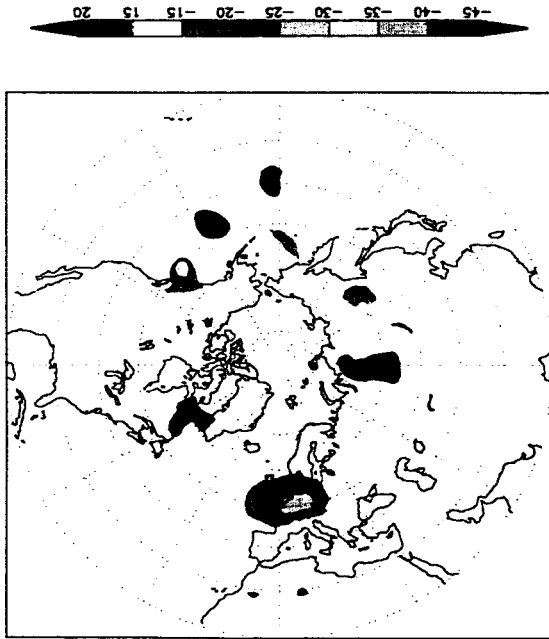
0013Jan 2004 NCEP Analyses



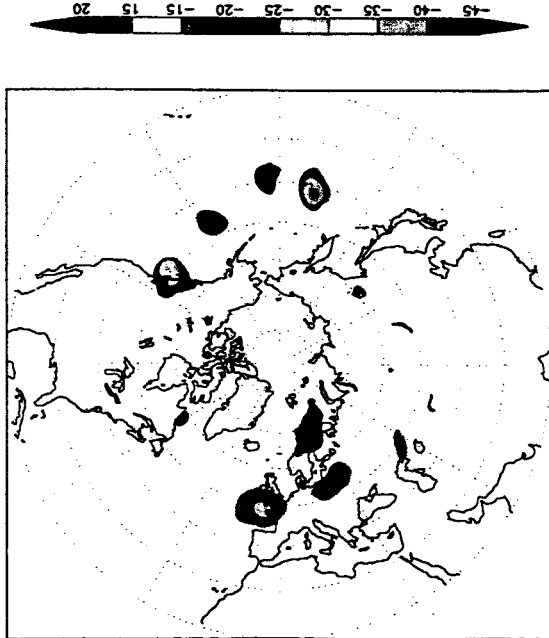
0013Jan 2004 AIRS Analyses



0013Jan 2004 Control Analyses



0013Jan 120h Fc minus An. (AIRS)



0013Jan 120h Fc minus An. (CNTRL)

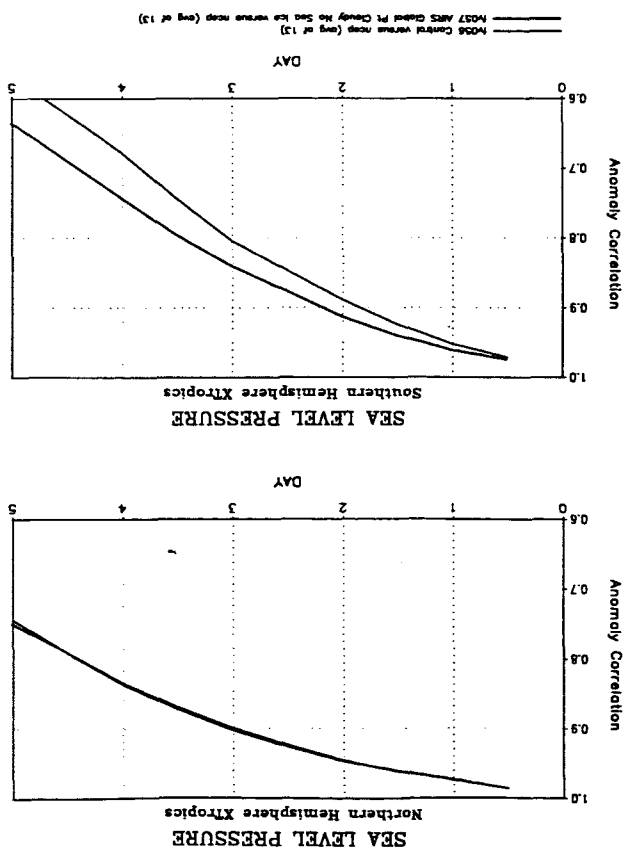
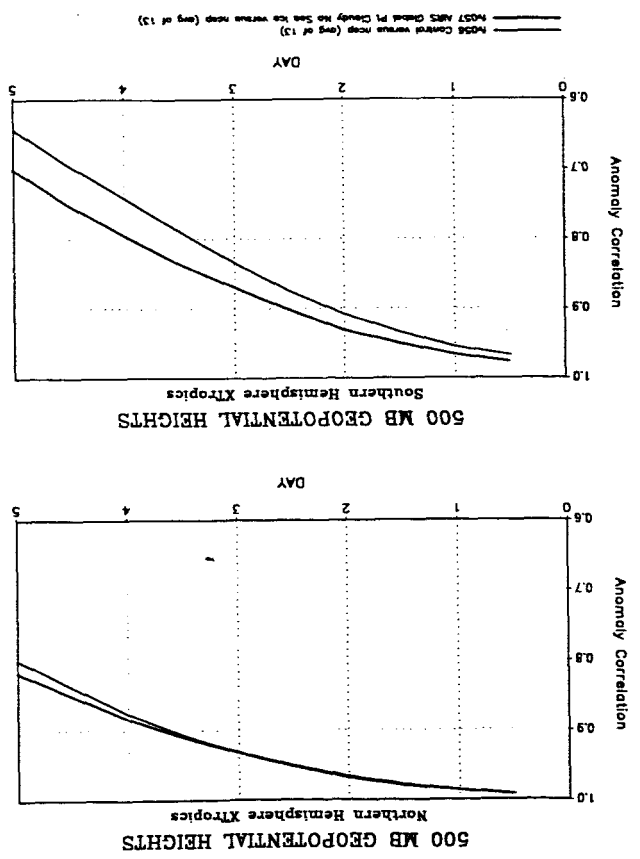


Figure 3. Sea level pressure anomaly correlation, calculated for latitudes between $30^{\circ}N$ and $80^{\circ}N$ (panel above) and $30^{\circ}S$ and $80^{\circ}S$ (below), with respect to NCEP verifying analyses. Black line: Control, red: AIRS.

Figure 4. 500 hPa geopotential height anomaly correlation, calculated for latitudes between 30°N and 80°N (panel above) and 30°S and 80°N (below), with respect to NCEP verifying analyses. Black line: Control, red: AIRS.



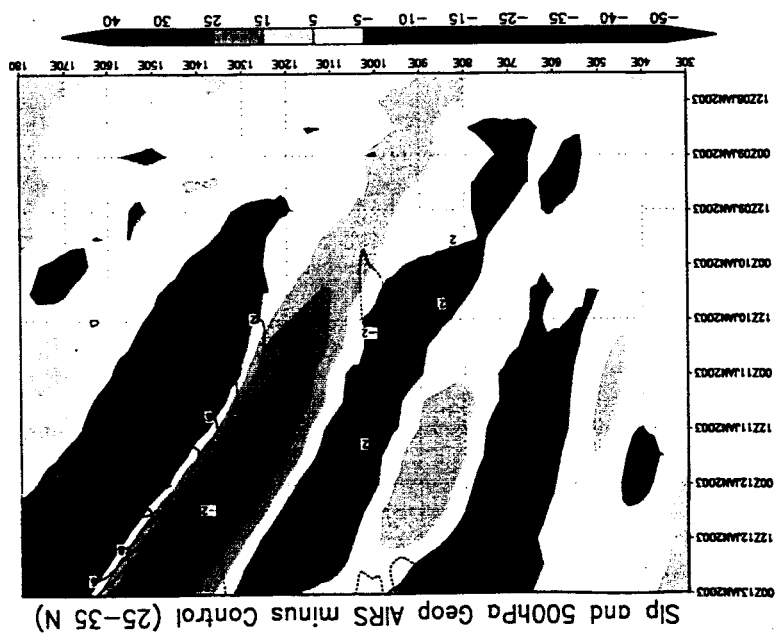


Figure 5. Hovmöller diagram of 500 height (m) and sea level pressure (hPa) anomaly (AIRS minus Control), averaged between 25°N and 35°N. Time increases upward.

Figure 6. 500 hPa (m) anomaly (AIRS minus Control) propagating from northern India (a) towards the Pacific (e, f). Note the amplification after 0000 UTC 10 January.

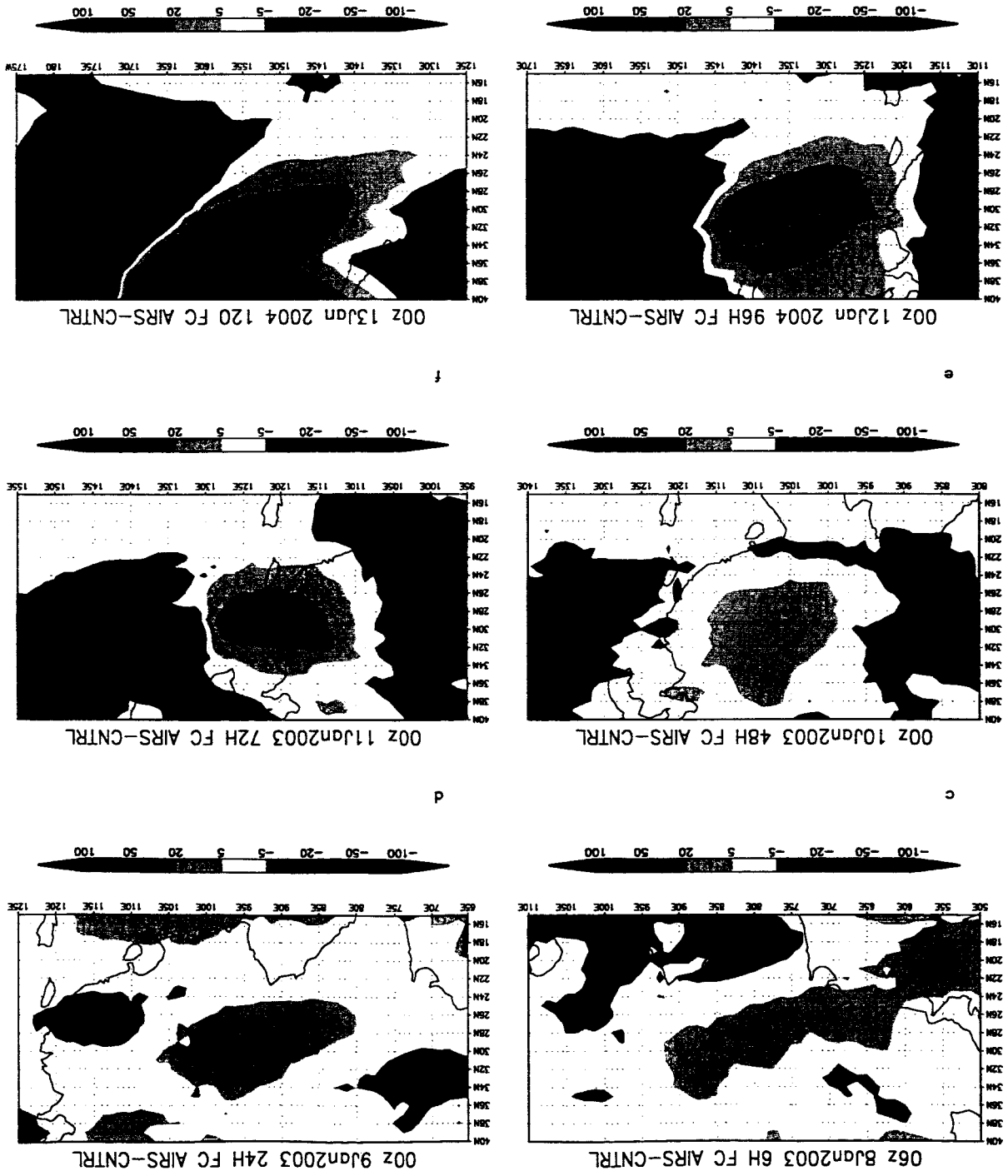
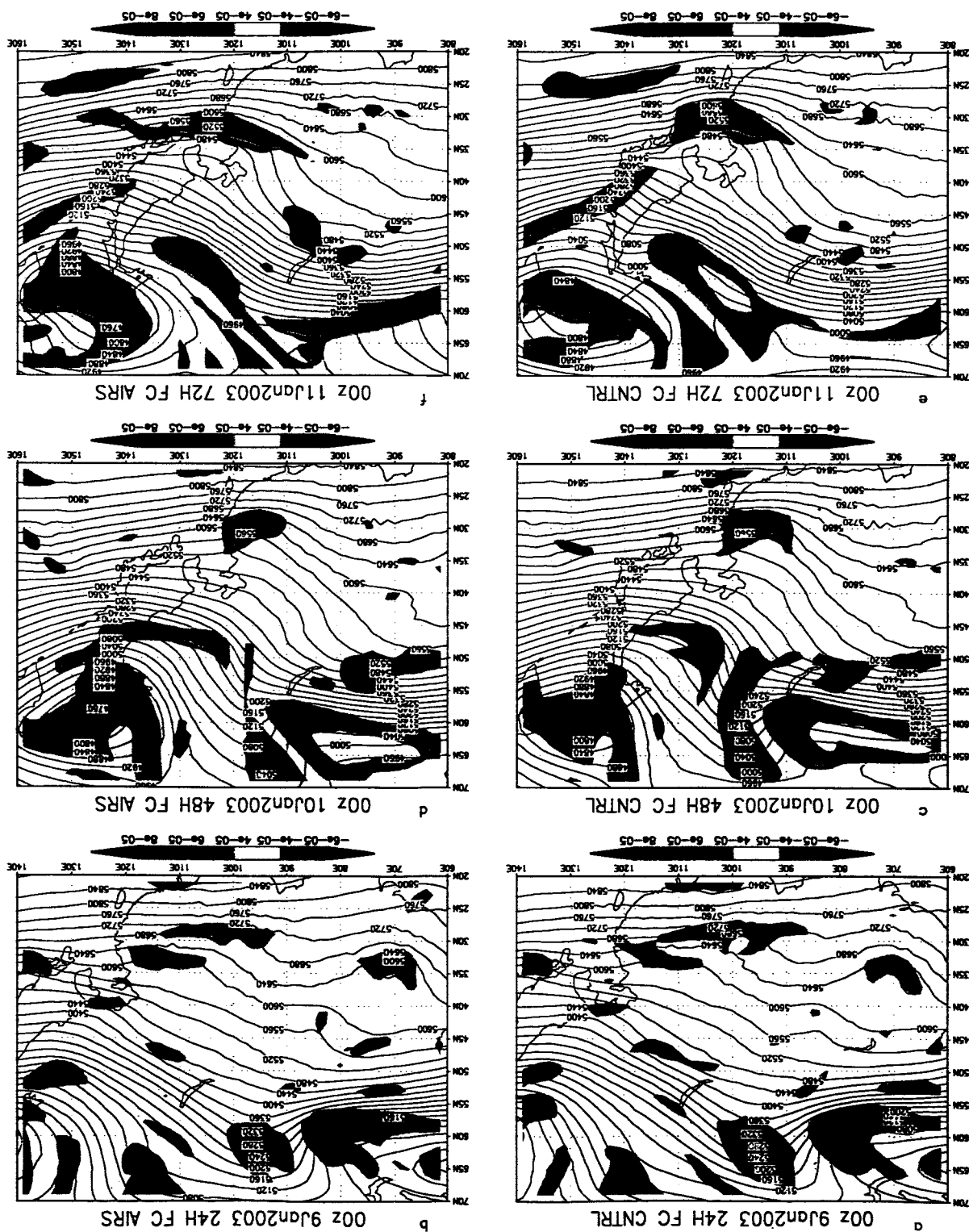


Figure 7. 500 hPa (m) and relative vorticity (s^{-1}). Left panels: Control. Right panels: AIRS.



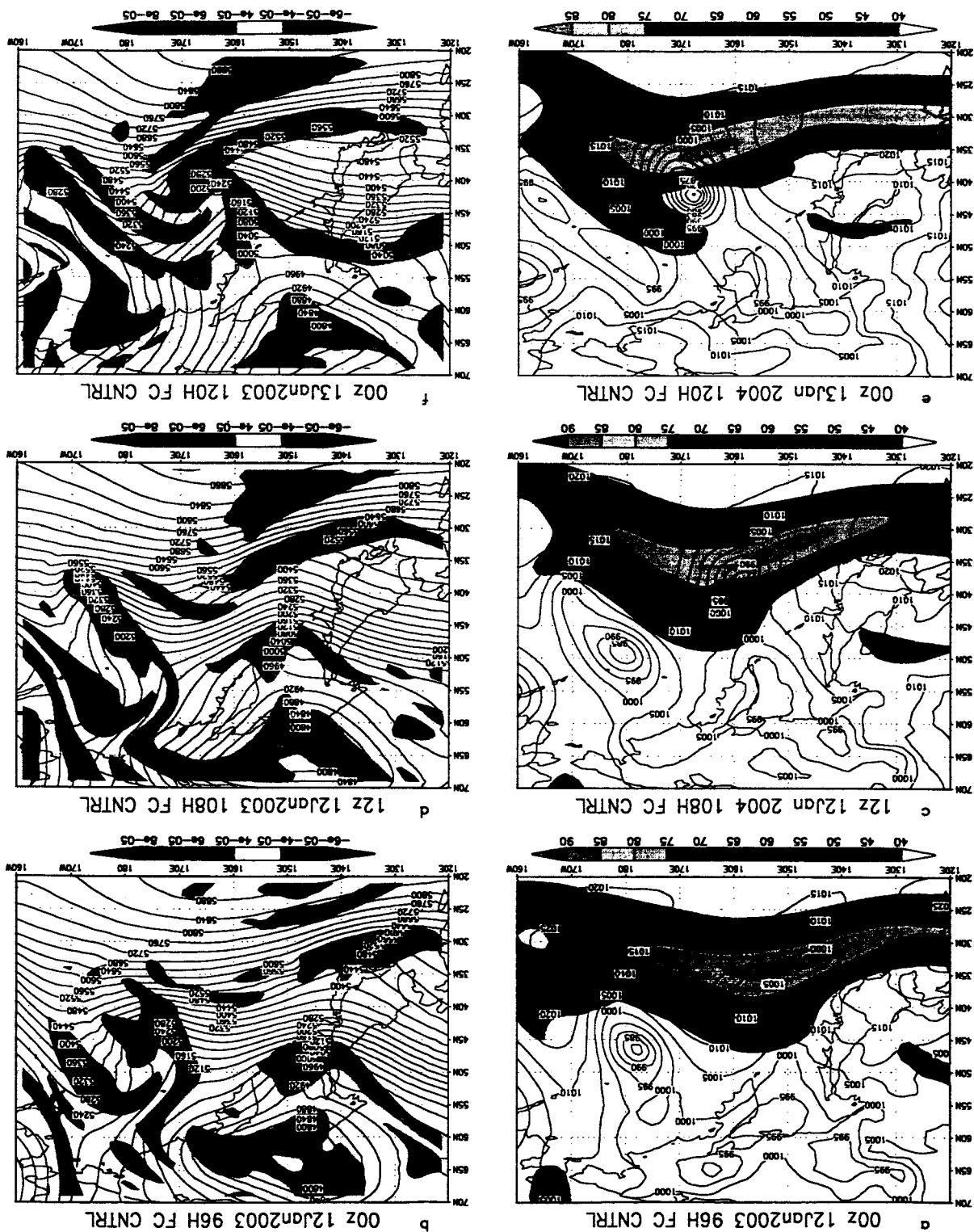


Figure 8. Left panels: control slip (hPa) and 250 hPa wind speed (ms^{-1}). Right panels: 500 hPa (m) and relative vorticity (s^{-1}).

Figure 9. Left panels: AIRS slip (hPa) and 250 hPa wind speed (ms^{-1}). Right panels: 500 hPa (m) and relative vorticity (s^{-1}).

